The Meteoritical Society

Meteoritics & Planetary Science 51, Nr 5, 906–919 (2016)
doi: 10.1111/maps.12634

Cluster analysis on the bulk elemental compositions of Antarctic stony meteorites

Hideaki MIYAMOTO[1,2,3*], Takafumi NIIHARA[1,4], Takeshi KURITANI[5], Peng K. HONG[1], James M. DOHM[1], and Seiji SUGITA[2]

[1]University Museum, University of Tokyo, 7-3-1 Hongo, Bunkyo-ku, Tokyo 113-0033, Japan
[2]Department of Earth and Planetary Sciences, University of Tokyo, 7-3-1 Hongo, Bunkyo-ku, Tokyo 113-0033, Japan
[3]Planetary Science Institute, 1700 East Fort Lowell, Suite 106, Tucson, Arizona 85719–2395, USA
[4]Lunar and Planetary Institute, Universities Space Research Association, 3600 Bay Area Boulevard, Houston, Texas 77058, USA
[5]Department of Natural History Sciences, Hokkaido University, N10W8 Kita-ku, Sapporo 060-0810, Japan
[*]Corresponding author. E-mail: hm@um.u-tokyo.ac.jp

(Received 16 December 2014; revision accepted 01 February 2016)

Abstract–Remote sensing observations by recent successful missions to small bodies have revealed the difficulty in classifying the materials which cover their surfaces into a conventional classification of meteorites. Although reflectance spectroscopy is a powerful tool for this purpose, it is influenced by many factors, such as space weathering, lighting conditions, and surface physical conditions (e.g., particle size and style of mixing). Thus, complementary information, such as elemental compositions, which can be obtained by X-ray fluorescence (XRF) and gamma-ray spectrometers (GRS), have been considered very important. However, classifying planetary materials solely based on elemental compositions has not been investigated extensively. In this study, we perform principal component and cluster analyses on 12 major and minor elements of the bulk compositions of 500 meteorites reported in the National Institute of Polar Research (NIPR), Japan database. Our unique approach, which includes using hierarchical cluster analysis, indicates that meteorites can be classified into about 10 groups purely by their bulk elemental compositions. We suggest that Si, Fe, Mg, Ca, and Na are the optimal set of elements, as this set has been used successfully to classify meteorites of the NIPR database with more than 94% accuracy. Principal components analysis indicates that elemental compositions of meteorites form eight clusters in the three-dimensional space of the components. The three major principal components (PC1, PC2, and PC3) are interpreted as (1) degree of differentiations of the source body (i.e., primitive versus differentiated), (2) degree of thermal effects, and (3) degree of chemical fractionation, respectively.

INTRODUCTION

Successful in situ observations of small bodies performed through spacecraft such as Galileo (e.g., Veverka et al. 1994), NEAR Shoemaker (e.g., Veverka et al. 2001), Rosetta (e.g., Keller et al. 2010; Sierks et al. 2011), and Dawn (e.g., Jaumann et al. 2012), as well as sample-return missions such as Stardust (e.g., Zolensky et al. 2006) and Hayabusa (e.g., Nakamura et al. 2011), increase the importance of studying meteorites more than ever. Meteorites are now determined to be precious samples from extraterrestrial bodies and thus identifications of the corresponding meteorite types of the targeted bodies of asteroid missions are among the major goals of asteroid missions. Besides such scientific importance, rapid identification of the surface materials during the reconnaissance phase is also critically important even for maneuvering a spacecraft. For example, when the Hayabusa spacecraft approached the targeted asteroid, Itokawa, obtaining appropriate information regarding surface materials was important in order to collect appropriate samples to optimize the science return (Fujiwara et al. 2006; Yano et al. 2006). A similar situation should occur in the future missions, such as Hayabusa 2 (Tsuda et al. 2013) and OSIRIS-Rex (Dworkin 2013).

The importance of identifying meteorites (or meteoroids) is not limited to small bodies. For example, on Mars, iron meteorites have been identified in Meridiani Planum by the Mars Exploration Rover (MER) Opportunity (Schroeder et al. 2008), due to exhumation of sedimentary deposits (Ashley et al. 2011; Fairen et al. 2011). On the basis of the larger meteorite flux and lower weathering rate expected on Mars, the estimated accumulation of meteorites on the surface of Mars (5×10^2–5×10^5/km^2 meteorites greater than 10 g) (Bland and Smith 2000) is far greater than on Earth. Therefore, even though MER identified two to three samples per square kilometer of traverse, which may seem like a large number, a far greater number of unidentified meteorites of likely large diversity should exist in the region explored by MER, considering factors such as size and possible obscuration by fine-grained materials. Prevalence of meteorites at the surface of Mars is evident through the Spirit and Opportunity discoveries (Schroeder et al. 2008).

MOTIVATION

Recent advances in reflectance spectrometry enable us to identify mineral compositions of surface materials of a target body by using spectrometers from close orbit. Modern spacecraft usually carry optical instruments, which often cover visible to infrared wavelengths for this purpose. However, irradiation by cosmic ray and solar wind, as well as bombardment by interplanetary dust particles, modify the surface of airless bodies through processes commonly referred to as space weathering (e.g., Pieters et al. 2000; Hapke 2001; Sasaki et al. 2002). This sometimes flattens or greatly changes the absorption characteristics of reflectance spectra (Sanchez et al. 2012). In fact, many asteroids are known to have featureless spectra with no absorption bands (including M- and D-type asteroids [Fornasier et al. 2010]), where identifications of surface materials purely by spectrometry can be challenging.

Difficulties in identifying surface materials by spectrometers could be made even more difficult if there is a mixture of different types of materials. An example is the petrologic complexity mapped on Vesta through the Dawn mission, which is interpreted to be due to a mixture of materials corresponding to howardite, eucrite, and diogenite (HED) meteorites (McSween et al. 2013). Surface heterogeneity of a small body may easily occur due to its small gravity (Miyamoto et al. 2007), which might be the reason for why the composition of Lutetia remains a puzzle even after the flyby of the Rosetta spacecraft; some regions seem to be similar to carbonaceous chondrites while the northern hemisphere could be similar to a mixture of enstatite and carbonaceous chondrites (Barucci et al. 2012). Another good example of particle mixtures is returned samples from the comet 81/P Wild 2, where an unexpected mixture of materials formed in different regions of a planetary disk (Brownlee et al. 2006). Furthermore, meteorites Kaidun and Sutter's Mill show assemblages of material ranging from CM to enstatite chondrites clasts, which have been interpreted to be the result of collisional formation of the parent body with different compositions such as E, D, and C types (Zolensky and Ivanov 2003; Zolensky et al. 2014); this implies that asteroids may be generally composed of mixtures of several different classes of meteorites.

Multiple approaches for identifying surface materials are, therefore, indispensable for interpreting remote-sensed data of both previous and future missions. However, we note that remote sensing of extraterrestrial bodies from space missions is significantly different from laboratory-based contemporary geochemical analyses of meteorites, where trace elements at the level of parts per billion even on single mineral grain can be measured; instruments onboard spacecraft are limited in terms of weight, power, and size. Also, current meteorite classifications are based on mineral composition and petrographical signatures, which are generally difficult to observe by remote sensing. In this sense, elemental compositions, which are obtained by onboard X-ray fluorescence (XRF) and gamma-ray spectrometers (GRS), can be adequately used for meteorite classification has been successfully shown by previous missions. For example, X-ray/gamma-ray instrument (XRGS) on-board NEAR Shoemaker was a critical instrument in identifying surface materials (Trombka et al. 2000); the elemental ratios of Eros's surface obtained through the mission were compared to a bulk elemental compositional database of meteorites (Nittler et al. 2001). This is reasonable because a bulk elemental composition is one of the most fundamental pieces of information about terrestrial rocks to both classify rock types and clarify their formational history (Harker 1909).

Given these situations, the motivations of this work is to understand (1) how well we can identify meteorite types based only on elemental compositions, (2) what kind of combinations of elements may be useful for classification, and (3) what is the least number of elements that can be used to accurately identify a meteorite. We focus our discussion on the bulk compositions of stony meteorites for the above objectives, while not attempting to illustrate a review of the elemental compositions or the origin and evolutionary histories of meteorites.

METHODS: NATIONAL INSTITUTE OF POLAR RESEARCH (NIPR) DATABASE OF BULK ELEMENTAL COMPOSITIONS OF METEORITE

A few databases of bulk meteorite elemental abundances have been compiled (Urey and Craig 1953; Jarosewich 1990; Nittler et al. 2004; Schaefer and Fegley 2010). Jarosewich compiled bulk chemical compositions of various types of meteorites, totaling 252 samples (Jarosewich 1990), which is useful for understanding the general trend of compositions for an individual meteorite class, particularly because the data are acquired using standard wet-chemistry techniques (Peck 1964; Jarosewich 1966). Similarly, using standard wet-chemistry techniques, Yanai and Kojima (1995) acquired bulk chemical compositions of Antarctic meteorites stored in the National Institute of Polar Research (NIPR), Japan. Nittler, who also compiled a database mostly based on these databases (Nittler et al. 2004), discussed inherent biases due to the analytical techniques, sample sizes, and intralaboratory systematic errors. Although the overall data ranges largely overlap between the databases, systematic offsets depending on laboratories exist and their exact cause remains uncertain (Nittler et al. 2004).

In this work, we use the NIPR database of meteorite bulk compositions (Yanai and Kojima 1995) for the following reasons (1) the database includes a total of 520 meteorites covering diverse types; (2) the bulk major elemental compositions of the database have been obtained using standard wet chemical analyses, so that a higher and consistent precision is expected (Peck 1964; Jarosewich, 1966); (3) all data are obtained and compiled by the same person (Mr. H. Haramura), where no intralaboratory biases are included in the database; (4) samples for the measurements were randomly selected from the entire collection of the Antarctic meteorites stored in NIPR, and thus, the database may be considered to nearly be a random sampling of the meteorite population found on the surface of the Earth except for iron meteorites.

Meteorite types, which have small populations, are not included in this data set due to the small number of items in the database (included only 1% of the entire meteorite samples of >50,000); most of these samples have small masses in which the bulk composition is difficult to measure anyway. Therefore, most of the major meteorite types such as ordinary chondrites, carbonaceous chondrites, enstatite chondrites, primitive achondrites, and achondrites (lunar and HED meteorites) are included in our investigation. A total of 500 stony meteorites are used in this work (Table 1); the original database contains data from 520 meteorites, but we removed 20 meteorites for the analysis of this work because they were classified as "unique" and/or "inclusion," and lack key elemental data.

Table 1. Population of each meteorite class in NIPR database.

Meteorite class	Number of sample	%
Acaplcoite	1	0.2
Lodranite	3	0.6
Angrite	1	0.2
Aubrite	2	0.4
Mesosiderite	2	0.4
Carbonaceous chondrite	30	5.8
Enstatite chondrite	6	1.2
H chondrite	165	31.7
L chondrite	161	31.0
LL chondrite	62	11.9
Anorthosite (lunar)	4	0.8
Basaltic lunar meteorite	3	0.6
Howardite	9	1.7
Eucrite	43	8.3
Diogenite	11	2.1
Shergottite (Mars)	1	0.2
Ureilite	9	1.7
Unique	4	0.8
Other (inclusion and clast in ordinary chondrite)	3	0.6
Total	520	100

Caveats of this analysis include (1) the existence of possible systematic errors involved in the original data set (the quality or reliability of the database is out of the scope of this paper); (2) alteration by weathering after the fall of a meteorite is not taken into account; and (3) the bulk elemental composition analysis should always be influenced by the heterogeneity of meteorites, which is not fully considered, as well as sampling biases. We note that our statistical analyses using the NIPR Antarctic meteorite database is performed here to show the general utility of the clustering analyses even with possible (but limited) inclusions of errors discussed above, rather than critically determining exact ranges of elements of each meteorite type.

RESULTS: STATISTICAL ANALYSIS ON BULK COMPOSITIONS OF METEORITES

Bulk compositional data of 12 elements (Table 2) are used in the statistical analyses: Si, Ti, Al, Fe, Mn, Mg, Ca, Na, K, P, Cr, and Ni (wt%). We perform hierarchical clustering analyses using Ward's minimum variance method (Ward 1963) based on the set of elements. This method minimizes the total variance between the clusters; the pair of clusters with minimum between-cluster distance is merged at each step, and thus finally the clusters with the largest distance are

Table 2. Summary of NIPR database of bulk elemental compositions of 500 meteorites.

	Si	Fe	Al	Mg	Ca	Na	Mn	K	P	Cr	Ti	Ni
Min	11.250	3.900	0.100	3.170	0.320	0.010	0.030	0.020	0.010	0.040	0.010	0.000
Mean	17.846	22.810	1.825	13.817	1.867	0.537	0.246	0.065	0.104	0.319	0.097	1.097
Median	17.830	22.805	1.295	14.625	1.240	0.580	0.240	0.070	0.100	0.300	0.050	1.155
Max	24.340	47.100	15.000	25.360	11.640	1.030	0.500	0.190	0.280	4.150	0.990	12.350
Std Dev	2.265	5.064	1.789	3.274	1.861	0.179	0.076	0.024	0.051	0.254	0.128	0.760

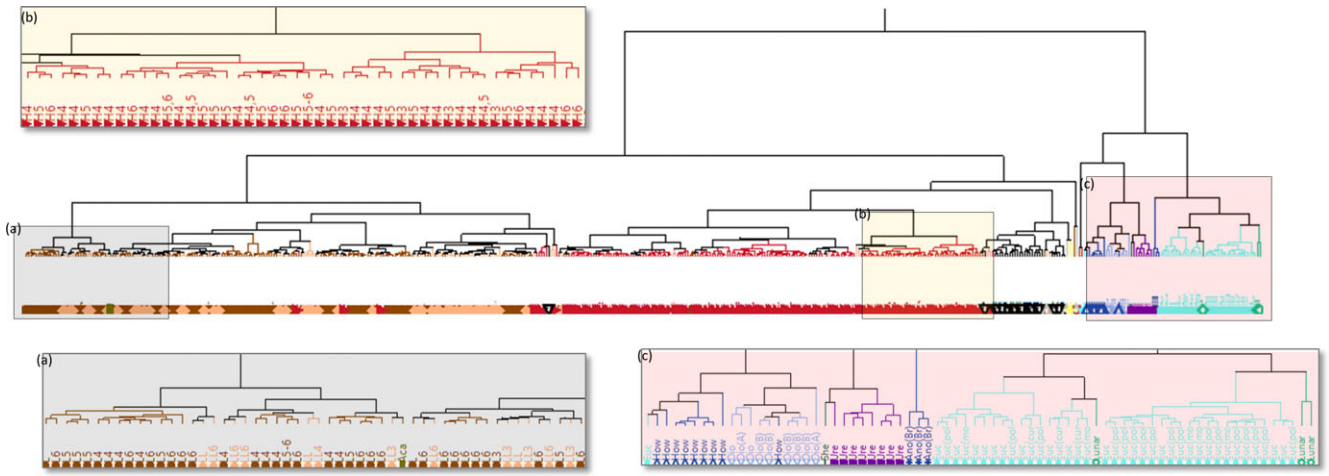

Fig. 1. Dendrogram resulted from the hierarchical clustering analysis of elementary composition database of NIPR meteorites by Ward method based on 12 elements. Because of the size of data (500 samples), the dendrogram is significantly shrunk with insets, which are close-ups of the original version. Full-scale version is available as online supporting material (Figure S1).

merged. Figure 1 (full version is in supporting information as Fig. S1) is the dendrogram, which illustrates how statistically close the meteorites and their clusters are in terms of their bulk elemental compositions. Because of the size of the dendrogram with 500 samples, we make a simplified version of the dendrogram, which is illustrated in Table 3. It shows that when we divide all meteorites into two groups, they either represent a relatively primitive group of meteorites (e.g., chondrites and primitive achondrites, such as acapulcoite and lodranite) or a relatively differentiated group of meteorites (e.g., lunar, Martian, and HED meteorites). Primitive groups are then classified into (1) carbonaceous chondrites with primitive achondrites, (2) enstatite (E) and H chondrites, and (3) L and LL chondrites with acapulcoite. Differentiated groups are classified as two large groups: crustal materials (lunar anorthosite, eucrite, and lunar meteorites [basaltic breccia]) and others (such as diogenite, howardite, and shergottite). Note that these classifications (from two large groups to much detailed classifications) are statistically obtained without any prejudice, although are generally reasonable compared to our understanding of meteorites.

We find that cluster analyses using bulk elemental compositions generally agree with conventional classification (Weisberg et al. 2006) on the basis of petrographical observations and mineral compositions at the level of class and clan. Surprisingly, the accuracy of the classification is pretty high; 94% of meteorites are successfully classified into groups consistent with classifications shown by Yanai and Kojima (1995). On the other hand, although we can distinguish E from H chondrites and lodranites from C chondrites when classified into 12 groups, the accuracy compared to the ordinary methods is reduced to below 70%.

We also find that the accuracy depends on a set of elements for the clustering analysis. Therefore, we perform a principal components analysis for the 12 elements noted above, to understand the overall characteristics of each element on delineated clusters. We obtain the loading matrix for the principal components 1, 2, and 3 (Table 4), whose percentages against the entire behavior are 45.6%, 12.7%, and 11.8%. When we illustrate components of PC1 and PC2, as shown in Fig. 2, we find that the representative elements in the first to the fourth quadrants in the plot are Si, Fe, Mg, and Ca. We also consider Na to be an

Table 3. Simplified version of the dendrogram (Figure 1) obtained from the hierarchial clustering analysis.

Clusters	2	3	4	5	6	7	8	9	10	11	12
Meteorite classes	Aca, C, E, H, L, LL, Lod, Mes	Aca, L, LL	Aca, L, LL	Aca, L, LL	Aca, L, LL	Aca, L, LL	Aca, L, LL	Aca, L, LL	Aca, LL	Aca, LL	Aca, LL
									L	L	L
		C, E, H, Lod, Mes	C, E, H, Lod, Mes	E, H	E, H	E,H	E,H	E,H	E,H	E,H	E
											H
				C, Lod, Mes	C, Lod, Mes	C,Lod	C,Lod	C,Lod	C,Lod	Lod	Lod
										C	C
						Mes	Mes	Mes	Mes	Mes	Mes
	Ano, Dio, Euc, How, Lunar, She,Ure	Ano, Dio, Euc, How, Lunar, She, Ure	Ano, Euc, Lunar	Ano, Euc, Lunar	Ano, Euc, Lunar	Ano, Euc, Lunar	Ano	Ano	Ano	Ano	Ano
							Euc, Lunar	Euc, Lunar	Euc, Lunar	Euc, Lunar	Euc, Lunar
			Dio, How, She,Ure	Dio, How, She,Ure	Dio, How	Dio, How	Dio, How	Dio	Dio	Dio	Dio
								How	How	How	How
					She,Ure	She, Ure	She, Ure	She, Ure	She, Ure	She, Ure	She, Ure
12 elements[a]	100%	96%	96%	95%	95%	94%	94%	94%	70%	82%	67%
5 elements[b]	99.60%	96%	96%	95%	95%	94%	94%	94%	84%	84%	62%
4 elements[c]	99.20%	94%	90%	90%	92%	92%	92%	92%	–	73%	70%
3 elements[d]	98%	93%	91%	88%	92%	92%	92%	76%	62%	62%	59%

[a]Accuracies of the classifications by clustering analyses against the original classifications using Si, Ti, Al, Fe, Mn, Mg, Ca, Na, K, P, Cr, and Na.
[b]Accuracies of the classifications by clustering analyses against the original classifications Si, Fe, Mg, Ca, and Na.
[c]Accuracies of the classifications by clustering analyses against the original classifications Si, Fe, Mg, and Ca.
[d]Accuracies of the classifications by clustering analyses against the original classifications Si, Fe, and Ca.
Aca, acapulcoite; C, carbonaceous; E, enstatite; H, H chondrite; L, L chondrite; LL, LL chondrite; Lod, lodranite; Mes, mesosiderite; Ano, lunar anorthosite; Dio, diogenite; Euc, eucrite; How, howardite; Luna, basaltic lunar meteorite; She, shergottite; Ure, ureilite.

Table 4. Loading matrix for the principal component 1, 2, and 3 resultant from the principal component analyses with 12 elements.

	PC1	PC2	PC3
Si	0.78399	0.43381	−0.15141
Fe	−0.7302	−0.29992	0.20118
Al	0.86644	−0.09366	0.35426
Mg	−0.80734	0.20339	−0.36936
Ca	0.93513	−0.06974	0.26934
Na	−0.49686	0.67125	0.41571
Mn	0.61513	0.31043	−0.3992
K	−0.40983	0.73826	0.34404
P	−0.36421	−0.06315	0.34593
Cr	−0.01819	0.20574	−0.64432
Ti	0.85373	0.04721	0.16741
Ni	−0.6237	−0.2197	0.0432

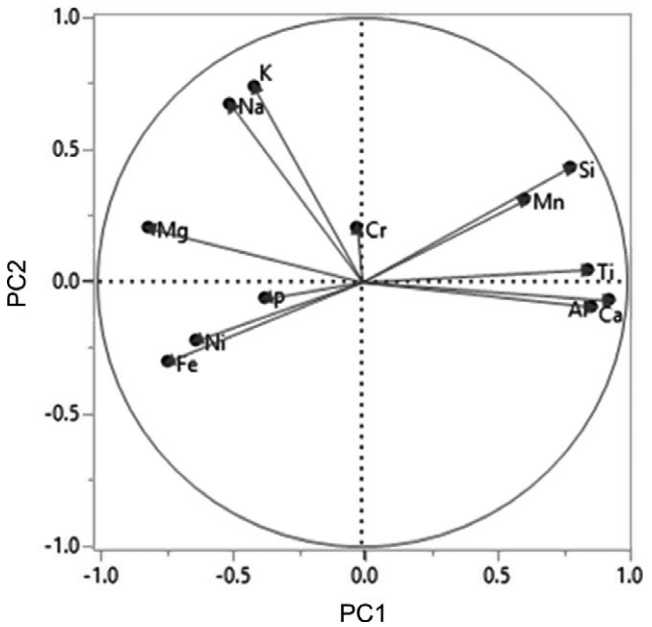

Fig. 2. Illustrative plot of the loading matrix of 12 elements on PC1 and PC2. The representative elements in the first to the fourth quadrants in the plot are Si, Fe, Mg, and Ca.

important element based on the loading matrix. Thus, we chose Si, Fe, Mg, Ca, and Na for our analyses detailed below. These elements were also chosen based on petrological reasons. For example, SiO_2 is the most abundant oxide in silicate rocks; Fe, Mg, and Ca are representative of basic elements that are abundant in mafic rocks; and Na is the major alkaline element and abundant in felsic rocks. Concentrations of these elements change during differentiation processes, and thus the elements are used to identify the compositional variation in terrestrial rocks (Harker 1909).

With this set of five elements (Si, Fe, Mg, Ca, and Na), the highest accuracy of statistical groupings compared to ordinary methods is obtained; sometimes the accuracy is higher than the cases in which the full set of 12 elements is used (Table 3). We interpret this to be the result of lower concentrations and variations in some elements (e.g., Ti and Cr) relative to other elements as well as of the smaller dispersions (lower standard deviations) for some of the other elements, such as K and P. In fact, the pairwise plots (Fig. 3) indicate that Cr and Ni contents do not correlate with other elements (correlations between elements are shown in Table 5). This is reasonable because these elements exist mostly in Fe-Ni metals, commonly found in undifferentiated meteorites such as chondritic meteorites. Siderophile elements are likely concentrated in the cores of differentiated parent bodies, and thus, those elements are poor in differentiated meteorites. In this sense, the Cr and Ni plots might reflect only those undifferentiated meteorites showing less variation. Although the accuracy for 10 clusters using Si, Fe, Mg, Ca, and Na is as high as 94%, it drops down to 77% when we use Si, Al, Fe, Mg, and K. Interestingly, a set of three elements, such as Si, Fe, and Ca, can sometimes show a decent accuracy (92% for eight clusters), which may be reasonable when considering the relatively similar performances of Mg to Fe and Na to Ca, and that they are representative elements in the first, second, and third quadrants in Fig. 2.

We further perform a flat clustering analysis using the k-means method, which finds the k-cluster centers, while assigning the objects to the nearest cluster center to minimize the squared distances from the cluster. We use the five elemental compositions selected above, whose elemental composition data are scaled individually. The resultant groups are (1) L and LL chondrites and acapulcoite, (2) E and H chondrites, (3) C chondrites and lodranites, (4) outliers, (5) anorthosites (lunar), (6) eucrites and basaltic lunar meteorites, (7) diogenites and howardites, and (8) shergottites and ureilites.

These clusters are illustrated in Fig. 4 as three biplots of PC1, PC2, and PC3. Even though some clusters appear to overlap each other in such a two-dimensional plot, when we plot the clusters on three-dimensional biplots using principal components 1, 2, and 3 as x, y, and z axes, these groups are clearly distinguished (Fig. 5). We find the correlations of principal components 1, 2, and 3 are 60.2, 19.5, and 14.7%, respectively. For a comparison, we also perform a flat clustering analysis using the k-means method with three elemental compositions (Si, Fe, and Ca), whose three-dimensional biplots are shown in the same way as Fig. 6. Interestingly, the resultant clusters are very similar to those obtained for five elemental compositions.

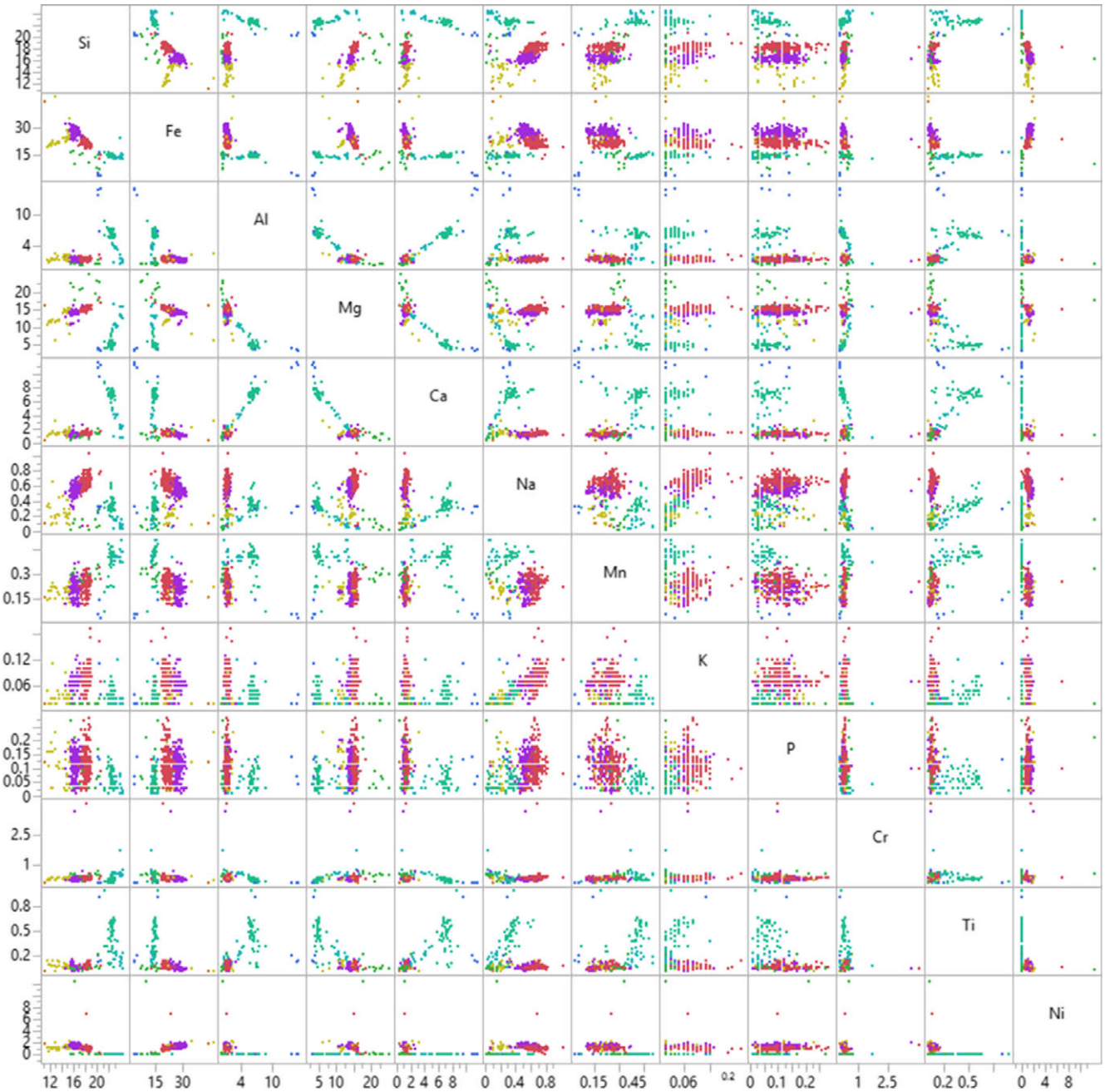

Fig. 3. Pairwise scatter plot of 12 elements in matrix. Each dot represents elemental composition of a meteorite. Colors correspond to eight clusters identified by k-means method (see main text). Lithophile elements shows largely distributed variation, while siderophile elements (Ni and Cr) show almost no correlation with other elements. Note that data of each meteorite seem to create clusters when we use any two elements except for siderophiles; however, clusters are overlapping each other and thus we could not really identify meteorite classes only from a pairwise plot.

DISCUSSION

Current meteorite classification is established through petrological and mineralogical observations, and mineral compositions. The number of meteorite types has increased to more than 70 with an increase in recent findings in both Antarctica and desert environments. In the case of chondrites, there are six different metamorphic types based on the heterogeneity of mineral compositions and mineral assemblages, which in turn forms the basis for classifying the grade of thermal metamorphism (Weisberg et al. 2006). Bulk major element compositions remain largely unchanged under early thermal metamorphism (by short-lived radio

Table 5. Correlations of 12 elements for 500 meteorites in the NIPR database.

	Si	Fe	Al	Mg	Ca	Na	Mn	K	P	Cr	Ti	Ni
Si	1	−0.75	0.571	−0.44	0.651	−0.16	0.664	−0.13	−0.26	0.092	0.604	−0.55
Fe	−0.75	1	−0.59	0.312	−0.61	0.266	−0.48	0.208	0.198	−0.13	−0.52	0.503
Al	0.571	−0.59	1	−0.85	0.961	−0.32	0.267	−0.29	−0.19	−0.13	0.711	−0.45
Mg	−0.44	0.312	−0.85	1	−0.89	0.349	−0.34	0.3	0.205	0.127	−0.78	0.355
Ca	0.651	−0.61	0.961	−0.89	1	−0.39	0.409	−0.32	−0.25	−0.11	0.823	−0.49
Na	−0.16	0.266	−0.32	0.349	−0.39	1	−0.27	0.739	0.265	−0.05	−0.33	0.21
Mn	0.664	−0.48	0.267	−0.34	0.409	−0.27	1	−0.16	−0.35	0.135	0.529	−0.35
K	−0.13	0.208	−0.29	0.3	−0.32	0.739	−0.16	1	0.082	−0.02	−0.22	0.163
P	−0.26	0.198	−0.19	0.205	−0.25	0.265	−0.35	0.082	1	−0.04	−0.23	0.213
Cr	0.092	−0.13	−0.13	0.127	−0.11	−0.05	0.135	−0.02	−0.04	1	−0.04	0.035
Ti	0.604	−0.52	0.711	−0.78	0.823	−0.33	0.529	−0.22	−0.23	−0.04	1	−0.46
Ni	−0.55	0.503	−0.45	0.355	−0.49	0.21	−0.35	0.163	0.213	0.035	−0.46	1

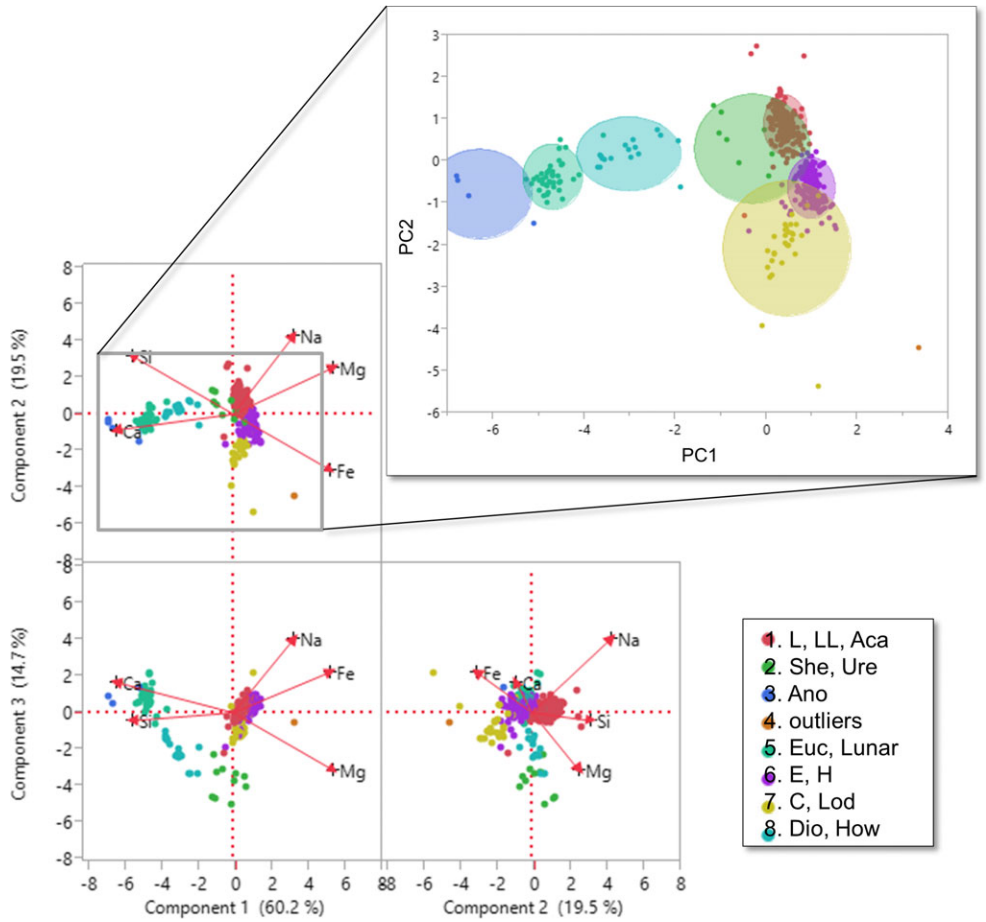

Fig. 4. Biplots of all of elemental composition data of 500 NIPR meteorites in three two-dimensional plots of PC1, PC2, and PC3. Points represent each meteorite with color representing each cluster. Inset is a close-up of the plot with PC1 and PC2 with distribution ellipses of clusters. Color represents each cluster.

isotope) that chondrites experienced, indicating it might be hard to obtain detailed classification in the same level with petrological and mineralogical classification from bulk chemical composition of meteorites. However, classification using detailed chemical data yields a different perspective, including revealing geologic events, as well as petrological information. Thus, combination of petrological and geochemical classification may help us to understand the petrogenesis of the rocks.

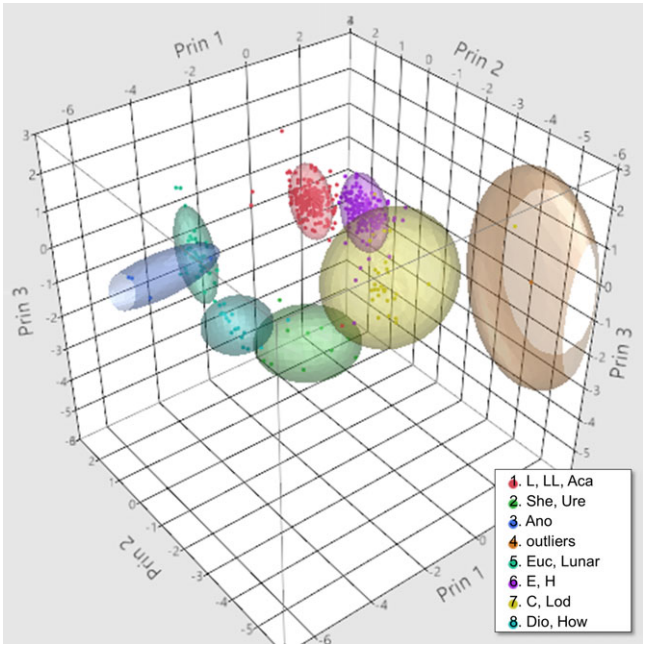

Fig. 5. 3-D plot of all of elemental composition data of 500 NIPR meteorites clustered by using five elements (Si, Fe, Mg, Ca, and Na). X, Y, and Z axes are PC1, PC2, and PC3. Points represent each meteorite with color representing each cluster.

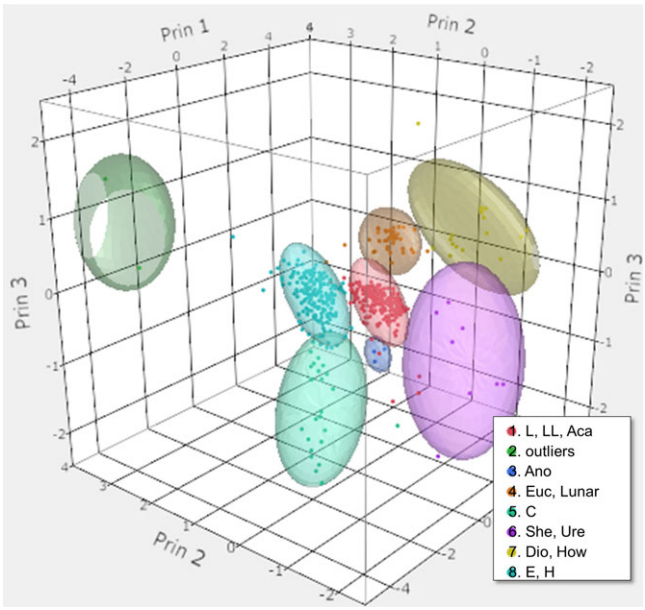

Fig. 6. 3-D plot of all of elemental composition data of 500 NIPR meteorites clustered by using three elements (Si, Fe, and Ca). X, Y, and Z axes are PC1, PC2, and PC3. Points represent each meteorite with color representing each cluster.

Multivariate cluster analyses on the bulk elemental composition data of the NIPR Antarctic meteorite database show that meteorites can be classified into eight groups based purely on their bulk elemental compositions. This is somewhat surprising because our clustering analyses are conducted without any petrological information such as presence of metals. Hierarchical cluster analyses indicate that meteorites can be largely classified into relatively primitive or differentiated groups. Each group can be further classified into smaller groups based on the elemental compositions, up to 12 groups, with reasonable accuracy (Table 3).

Meteorite samples in the relatively primitive group discussed above contain abundant Fe-Ni metal and sulfide materials. Mesosiderites are thought to have formed by mixing of a lithic crust from a differentiated body and Fe-Ni metals (Hewins 1984). The relatively differentiated group experienced metal/silicate segregation during differentiation on the Moon, Mars, and HED parent body (probably asteroid Vesta). One type of a primitive achondrite, ureilites, has achondritic signatures in their mineralogy, petrological textures, and bulk compositions with low amount of Fe-Ni metals. Although petrogenesis of this meteorite group is not well understood (Mittlefehldt et al. 1996; Goodrich et al. 2004), these meteorites are classified close to an achondritic meteorite in this statistic work, at least being distinguished from other primitive achondrites (acapulcoites and lodranites). Acapulcoites and lodranites have similar mineral assemblage with chondrite, thus our clustering result is consistent with mineralogical classification. Distinction between acapulcoites and lodranites is not clear. Moreover, there are intermediate meteorites between acapulcoites and lodranites such as Elephant Moraine (EET) 84302 (Takeda et al. 1994; McCoy et al. 1997a, 1997b; Mittlefehldt et al. 1998). The NIPR meteorite catalog (Yanai and Kojima 1995) contains very limited numbers of acapulcoite and lodranites, which might be endmembers, while not containing an intermediate meteorite, thus the two meteorites separated into different groups in an early stage of clustering.

Principal component analysis shows that a set of elements, such as Si, Fe, Mg, Ca, and Na, can result in clusters with generally good agreement with those determined through traditional (petrological–mineralogical) classifications. We consider that the selection of these elements is supported by our standard knowledge of petrology and geochemistry of meteorites. Generally bulk elemental composition varies continuously with changing mineral crystallization sequences under differentiation process. Therefore, binary plots of Si versus other major elements (in oxides; Harker diagram) are commonly used for identification of compositional variation. Bulk compositions also change during fractional

Table 6. Statistical range of each element for each cluster.

Elements	Statistics	1	2	3	4	5	6	7	8
Si	Min	16.95	15.52	20.12	–	21.20	14.72	11.76	22.66
	Mean	18.25	18.15	20.35	–	22.40	16.32	13.95	23.58
	Median	18.23	18.17	20.28	–	22.47	16.31	14.58	23.84
	Std Dev	0.46	1.85	0.28	–	0.40	0.48	1.22	0.56
	Max	20.58	20.31	20.73	–	23.14	17.60	15.47	24.34
Fe	Min	13.26	7.43	3.90	–	10.88	22.72	19.50	12.99
	Mean	21.63	13.05	7.54	–	14.73	27.47	24.40	14.58
	Median	21.77	14.36	4.80	–	14.78	27.53	22.81	13.84
	Std Dev	1.65	3.52	6.12	–	0.98	1.76	5.40	2.67
	Max	25.61	17.25	16.65	–	16.88	32.27	47.10	24.45
Mg	Min	13.88	17.81	3.17	–	3.62	10.65	6.04	9.61
	Mean	15.38	21.32	3.45	–	4.95	14.11	12.58	12.50
	Median	15.37	21.43	3.44	–	4.73	14.14	12.26	12.69
	Std Dev	0.45	2.42	0.24	–	1.06	0.62	2.22	2.16
	Max	18.51	25.36	3.75	–	8.68	16.27	15.37	16.68
Ca	Min	1.01	0.39	9.47	–	5.11	0.64	0.74	0.79
	Mean	1.29	1.05	10.83	–	7.10	1.17	1.48	2.79
	Median	1.28	1.03	11.11	–	7.18	1.14	1.42	2.51
	Std Dev	0.13	0.48	0.95	–	0.68	0.21	0.44	1.27
	Max	1.99	2.03	11.64	–	8.78	2.61	3.14	4.70
Na	Min	0.07	0.01	0.24	–	0.19	0.07	0.09	0.03
	Mean	0.66	0.10	0.30	–	0.35	0.54	0.26	0.11
	Median	0.66	0.09	0.32	–	0.34	0.54	0.22	0.10
	Std Dev	0.08	0.08	0.04	–	0.09	0.08	0.13	0.05
	Max	1.03	0.27	0.33	–	0.63	0.72	0.65	0.19

crystallization sequences. Constituent rock-forming minerals are separated into two types, mafic and felsic minerals. Mafic minerals, olivine and pyroxene, are rich in Fe and Mg, while felsic minerals, such as plagioclase, contain abundant Na and Ca. These minerals are also common in meteorites (except for iron meteorites). Mg-rich mafic minerals generally crystallize in the early stage (at high temperature), and residual melt composition changes toward Fe-rich composition. In the same way, Ca-rich plagioclase crystallized prior to Na-rich plagioclase with the residual melt being rich in Na. These sequences are gradually changed because most of minerals have a solid solution. Silicon is the fundamental element and abundant in silicate melt. The abundance of Si in the residual melt increases during differentiation/fractionation.

Our principal component analysis using the set of five elements (Si, Fe, Mg, Ca, and Na) shows that the eigenvectors for the principal component 1 (PC1) are Si (−0.46), Fe (0.45), Mg (0.46), Ca (−0.54), and Na (0.28), which imply that all four elements except for Na are almost equally important for PC1. On a biplot on PC1 and PC2 (Fig. 4), we find that the order of the values of PC1 are groups 3 (lunar anorthosites), 5 (eucrites and basaltic lunar meteorites), 8 (diogenites and howardites), 1 (L and LL chondrites and acapulcoites), 6 (E and H chondrites), and 7 (C chondrites and lodranites). We thus interpret that the PC1 is a good indicator of the degree of differentiations of the source body (i.e., primitive versus differentiated). Eigenvectors of PC2 are Si (0.47), Fe (−0.45), Mg (0.37), Ca (−0.13), and Na (0.64), indicating that Na is the most dominant element and Si, Fe, and Mg also play significant roles. The values of PC2 is higher for group 1 (L and LL chondrites and acapulcoites) and lower for group 7 (C chondrites and lodranites). These may indicate thermal conditions during formation and/or shock annealing of meteorites, where Na and the state of major silicate minerals such as olivine and pyroxene may largely contribute to PC2. Eigenvectors of PC3 are Si (−0.07), Fe (0.38), Mg (−0.53), Ca (0.29), and Na (0.69), implying that the effect of Na is dominant with effects of Mg and Fe. We interpret this as an indicator of fractionations, which may be captured by Fe and Mg for mafic minerals and Na for felsic minerals, or may suggest that PC3 mainly represents the variation in the ratio of refractory elements relative to Na reflecting different source materials.

The statistical range of each element for each cluster is summarized in Table 6. We note that when we compare these results to other databases or meteorites not listed in the NIPR database, intralaboratory bias can be an issue as pointed out by Nittler et al. (2004), and thus, we are aware that the exact values of the

ranges may need to be modified. Nevertheless, when we apply these values to the Jarosewich database of bulk elemental compositions (Jarosewich 1990), we find that about 80% of meteorites are still properly classified. When we use the hierarchical clustering analyses by Ward's minimum variance method and the flat clustering analysis using the k-means method as discussed above to Jarosewich database, we find that, again, we can classify meteorites into as many as 8–12 groups with the accuracy ranging from 94 to 84%, respectively, with the same set of element such as Si, Fe, Mg, Ca, and Na. This indicates that, although the exact range of each element may be modified, rough and quick classification of meteorites is possible based only on their elemental compositions.

CONCLUSIVE REMARKS

Statistical classification using bulk major element composition presented in this work can approximately reproduce current classification schemes based on petrology, mineralogy, and mineral chemistry on the level of "class to clan" (Weisberg et al. 2006). The "group level" is difficult to determine using bulk composition because this classification is highly dependent on petrological observation in addition to rarity of homogeneous meteorites (most meteorites have experienced impact events and show brecciated texture). When we classify into more than nine clusters, the number of outliers increases whereas the accuracy decreases. Thus, we conclude that a statistical classification through bulk major element compositions can be used to classify up to the "class" level. Importantly, while the presented classifications are results of statistical analysis of elemental compositions alone, the first classifications into two groups and further detailed groupings up to about 10 groups are generally consistent with our conventional classifications and understanding of meteorites.

We propose that a set of five elements, Si, Fe, Mg, Ca, and Na, is a more useful combination for classifying meteorites than 12 elements. We also find that removing Na from the set does not significantly affect the accuracy of the classifications; thus, elemental compositions of only Si, Fe, Ca, and Mg are useful to classify meteorites to the "class" level with a decent accuracy. For a further simplification, we recommend using Si, Fe, and Ca, which provides a similar accuracy level to using five elements at least for the analysis of the NIPR database. We note that the abundances of these elements are relatively easier to measure even by instruments onboard spacecraft.

While the intention of this work is to understand the availability of the bulk elemental composition data obtained in space, the results have important implications concerning field-based identification of meteorites on Earth. Usually, meteorites on Earth are found through their distinct appearance such as their dark color contrasting with the lighter Antarctic ice field and desert materials. However, thanks to the increasing availability of portable devices such as portable XRFs (e.g., TITAN of Bruker and DELTA of Olympus), which allow the determination of elemental abundances in the field, our new technique may lead to a much greater number of meteorites being discovered and collected over time (e.g., deserts where there is relatively low vegetation).

Acknowledgments—We are grateful to Dr. Zolensky (associate editor) for editorial handling. Constructive comments from Dr. Fairén and M. Ramy El-Maarry improve the manuscript. This work is supported in part by JSPS grant-in-aid 25120006 and TeNQ/Tokyo-dome.

Editorial Handling—Dr. Michael Zolensky

REFERENCES

Ashley J. W., Golombek M. P., Christensen P. R., Squyres S. W., McCoy T. J., Schroder C., Fleischer I., Johnson J. R., Herkenhoff K. E., and Parker T. J. 2011. Evidence for mechanical and chemical alteration of iron-nickel meteorites on Mars: Process insights for Meridiani Planum. *Journal of Geophysical Research-Planets* 116: E00F20. doi:10.1029/2010JE003672.

Barucci M. A., Belskaya I. N., Fornasier S., Fulchignoni M., Clark B. E., Coradini A., Capaccioni F., Dotto E., Birlan M., Leyrat C., Sierks H., Thomas N., and Vincent J. B. 2012. Overview of Lutetia's surface composition. *Planetary and Space Science* 66:23–30.

Bland P. A. and Smith T. B. 2000. Meteorite accumulations on Mars. *Icarus* 144:21–26.

Brownlee D., Tsou P., Aleon J., Alexander C. M. O., Araki T., Bajt S., Baratta G. A., Bastien R., Bland P., Bleuet P., Borg J., Bradley J. P., Brearley A., Brenker F., Brennan S., Bridges J. C., Browning N. D., Brucato J. R., Bullock E., Burchell M. J., Busemann H., Butterworth A., Chaussidon M., Cheuvront A., Chi M. F., Cintala M. J., Clark B. C., Clemett S. J., Cody G., Colangeli L., Cooper G., Cordier P., Daghlian C., Dai Z. R., D'Hendecourt L., Djouadi Z., Dominguez G., Duxbury T., Dworkin J. P., Ebel D. S., Economou T. E., Fakra S., Fairey S. A. J., Fallon S., Ferrini G., Ferroir T., Fleckenstein H., Floss C., Flynn G., Franchi I. A., Fries M., Gainsforth Z., Gallien J. P., Genge M., Gilles M. K., Gillet P., Gilmour J., Glavin D. P., Gounelle M., Grady M. M., Graham G. A., Grant P. G., Green S. F., Grossemy F., Grossman L., Grossman J. N., Guan Y., Hagiya K., Harvey R., Heck P., Herzog G. F., Hoppe P., Horz F., Huth J., Hutcheon I. D., Ignatyev K., Ishii H., Ito M., Jacob D., Jacobsen C., Jacobsen S., Jones S., Joswiak D., Jurewicz A., Kearsley A. T., Keller L. P., Khodja H., Kilcoyne A. L. D., Kissel J., Krot A., Langenhorst F., Lanzirotti A., Le L., Leshin L. A., Leitner J., Lemelle L., Leroux H., Liu M. C.,

Luening K., Lyon I., MacPherson G., Marcus M.A., Marhas K., Marty B., Matrajt G, McKeegan K., Meibom A., Mennella V., Messenger K., Messenger S., Mikouchi T., Mostefaoui S., Nakamura T., Nakano T., Newville M., Nittler L.R., Ohnishi I., Ohsumi K., Okudaira K., Papanastassiou D.A., Palma R., Palumbo M.E., Pepin R.O., Perkins D., Perronnet M., Pianetta P., Rao W., Rietmeijer F.J.M., Robert F., Rost D., Rotundi A., Ryan R., Sandford S.A., Schwandt C.S., See T.H., Schlutter D., Sheffield-Parker J., Simionovici A., Simon S., Sitnitsky I., Snead C.J., Spencer M.K., Stadermann F.J., Steele A., Stephan T., Stroud R., Susini J., Sutton S.R., Suzuki Y., Taheri M., Taylor S., Teslich N., Tomeoka K., Tomioka N., Toppani A., Trigo-Rodríguez J.M., Troadec D., Tsuchiyama A., Tuzzolino A.J., Tyliszczak T., Uesugi K., Velbel M., Vellenga J., Vicenzi E., Vincze L., Warren J., Weber I., Weisberg M., Westphal A.J., Wirick S., Wooden D., Wopenka B., Wozniakiewicz P., Wright I., Yabuta H., Yano H., Young E.D., Zare R.N., Zega T., Ziegler K., Zimmerman L., Zinner E., and Zolensky M. 2006. Research article—Comet 81P/Wild 2 under a microscope. *Science* 314:1711–1716.

Dworkin J. P. 2013. OSIRIS-REx will return a sample of asteroid 1999 RQ36 for astrochemistry. *Abstracts of Papers of the American Chemical Society* 246.

Fairen A. G., Dohm J. M., Baker V. R., Thompson S. D., Mahaney W. C., Herkenhoff K. E., Rodriguez J. A. P., Davila A. F., Schulze-Makuch D., El Maarry M. R., Uceda E. R., Amils R., Miyamoto H., Kim K. J., Anderson R. C., and McKay C. P. 2011. Meteorites at Meridiani Planum provide evidence for significant amounts of surface and near-surface water on early Mars. *Meteoritics & Planetary Science* 46:1832–1841.

Fornasier S., Clark B. E., Dotto E., Migliorini A., Ockert-Bell M., and Barucci M. A. 2010. Spectroscopic survey of M-type asteroids. *Icarus* 210:655–673.

Fujiwara A., Kawaguchi J., Yeomans D. K., Abe M., Mukai T., Okada T., Saito J., Yano H., Yoshikawa M., Scheeres D. J., Barnouin-Jha O., Cheng A. F., Demura H., Gaskell R. W., Hirata N., Ikeda H., Kominato T., Miyamoto H., Nakamura A. M., Nakamura R., Sasaki S., and Uesugi K. 2006. The rubble-pile asteroid Itokawa as observed by Hayabusa. *Science* 312:1330–1334.

Goodrich C. A., Scott E. R. D., and Fioretti A. M. 2004. Ureilitic breccias: Clues to the petrologic structure and impact disruption of the ureilite parent asteroid. *Chemie der Erde—Geochemistry* 64:283–327.

Hapke B. 2001. Space weathering from Mercury to the asteroid belt. *Journal of Geophysical Research-Planets* 106:10,039–10,073.

Harker A. 1909. *The natural history of igneous rocks*. New York: Macmillam. pp. xvi, 384 p. 2 leaves of plates.

Hewins R. H. 1984. Impact versus internal origins form mesosiderites. *Journal of Geophysical Research* 88:B257–B266.

Jarosewich E. 1990. Chemical-analyses of meteorites—A compilation of stony and iron meteorite analyses. *Meteoritics* 25:323–337.

Jarosewich E. 1966. Chemical analyses of ten stony meteorites. *Geochimica et Cosmochimica Acta* 30:1261–1265.

Jaumann R., Williams D. A., Buczkowski D. L., Yingst R. A., Preusker F., Hiesinger H., Schmedemann N., Kneissl T., Vincent J. B., Blewett D. T., Buratti B. J., Carsenty U., Denevi B. W., De Sanctis M. C., Garry W. B., Keller H. U., Kersten E., Krohn K., Li J. Y., Marchi S., Matz K. D., McCord T. B., McSween H. Y., Mest S. C., Mittlefehldt D. W., Mottola S., Nathues A., Neukum G., O'Brien D. P., Pieters C. M., Prettyman T. H., Raymond C. A., Roatsch T., Russell C. T., Schenk P., Schmidt B. E., Scholten F., Stephan K., Sykes M. V., Tricarico P., Wagner R., Zuber M. T., and Sierks H. 2012. Vesta's shape and morphology. *Science* 336:687–690.

Keller H. U., Barbieri C., Koschny D., Lamy P., Rickman H., Rodrigo R., Sierks H., A'Hearn M. F., Angrilli F., Barucci M. A., Bertaux J. L., Cremonese G., Da Deppo V., Davidsson B., De Cecco M., Debei S., Fornasier S., Fulle M., Groussin O., Gutierrez P. J., Hviid S. F., Ip W. H., Jorda L., Knollenberg J., Kramm J. R., Kuhrt E., Kuppers M., Lara L. M., Lazzarin M., Moreno J. L., Marzari F., Michalik H., Naletto G., Sabau L., Thomas N., Wenzel K. P., Bertini I., Besse S., Ferri F., Kaasalainen M., Lowry S., Marchi S., Mottola S., Sabolo W., Schroder S. E., Spjuth S., and Vernazza P. 2010. E-Type Asteroid (2867) Steins as imaged by OSIRIS on Board Rosetta. *Science* 327:190–193.

McCoy T. J., Keil K., Clayton R. N., Mayeda T. K., Bogard D. D., Garrison D. H., and Wieler R. 1997a. A petrologic and isotopic study of lodranites: Evidence for early formation as partial melt residues from heterogeneous precursors. *Geochimica Et Cosmochimica Acta* 61:623–637.

McCoy T. J., Keil K., Muenow D. W., and Wilson L. 1997b. Partial melting and melt migration in the acapulcoite-lodranite parent body. *Geochimica Et Cosmochimica Acta* 61:639–650.

McSween H. Y., Binzel R. P., De Sanctis M. C., Ammannito E., Prettyman T. H., Beck A. W., Reddy V., Le Corre L., Gaffey M. J., McCord T. B., Raymond C. A., Russell C. T., and Team D. S. 2013. Dawn; the Vesta-HED connection; and the geologic context for eucrites, diogenites, and howardites. *Meteoritics & Planetary Science* 48:2090–2104.

Mittlefehldt D. W., Lindstrom M. M., Bogard D. D., Garrison D. H., and Field S. W. 1996. Acapulco- and Lodran-like achondrites: Petrology, geochemistry, chronology, and origin. *Geochimica et Cosmochimica Acta* 60:867–882.

Mittlefehldt D. W., McCoy T. J., Goodrich C. A., and Kracher A. 1998. Non-chondritic meteorites from asteroidal bodies. *Planetary Materials* 36:D1–D195.

Miyamoto H., Yano H., Scheeres D. J., Abe S., Barnouin-Jha O., Cheng A. F., Demura H., Gaskell R. W., Hirata N., Ishiguro M., Michikami T., Nakamura A. M., Nakamura R., Saito J., and Sasaki S. 2007. Regolith migration and sorting on asteroid Itokawa. *Science* 316:1011–1014.

Nakamura T., Noguchi T., Tanaka M., Zolensky M. E., Kimura M., Tsuchiyama A., Nakato A., Ogami T., Ishida H., Uesugi M., Yada T., Shirai K., Fujimura A., Okazaki R., Sandford S. A., Ishibashi Y., Abe M., Okada T., Ueno M., Mukai T., Yoshikawa M., and Kawaguchi J. 2011. Itokawa dust particles: A direct link between S-type asteroids and ordinary chondrites. *Science* 333:1113–1116.

Nittler L. R., Starr R. D., Lim L., McCoy T. J., Burbine T. H., Reedy R. C., Trombka J. I., Gorenstein P., Squyres S. W., Boynton W. V., McClanahan T. P., Bhangoo J. S., Clark P. E., Murphy M. E., and Killen R. 2001. X-ray fluorescence measurements of the surface elemental composition of asteroid 433 Eros. *Meteoritics & Planetary Science* 36:1673–1695.

Nittler L. R., McCoy T. J., Clark P. E., Murphy M. E., Trombka J. I., and Jarosewich E. 2004. Bulk element compositions of meteorites: A guide for interpreting remote-sensing geochemical measurements of planets and asteroids. *Antarctic Meteorite Research* 17:233–253.

Peck L.C. 1964. Systematic analysis of silicates. *U. S. Geological Survey Bulletin* 1170, pp.89.

Pieters C. M., Taylor L. A., Noble S. K., Keller L. P., Hapke B., Morris R. V., Allen C. C., McKay D. S., and Wentworth S. 2000. Space weathering on airless bodies: Resolving a mystery with lunar samples. *Meteoritics & Planetary Science* 35:1101–1107.

Sanchez J. A., Reddy V., Nathues A., Cloutis E. A., Mann P., and Hiesinger H. 2012. Phase reddening on near-Earth asteroids: Implications for mineralogical analysis, space weathering and taxonomic classification. *Icarus* 220:36–50.

Sasaki S., Hiroi I., Nakamura K., Hamabe Y., Kurahashi E., and Yamada M. 2002. Simulation of space weathering by nanosecond pulse laser heating: Dependence on mineral composition, weathering trend of asteroids and discovery of nanophase iron particles. *Modelling and Laboratory Studies Supporting Space Missions to Small Bodies* 29:783–788.

Schaefer L. and Fegley B. 2010. Volatile element chemistry during metamorphism of ordinary chondritic material and some of its implications for the composition of asteroids. *Icarus* 205:483–496.

Schroeder C., Rodionov D. S., McCoy T. J., Jolliff B. L., Gellert R., Nittler L. R., Farrand W. H., Johnson J. R., Ruff S. W., Ashley J. W., Mittlefehldt D. W., Herkenhoff K. E., Fleischer I., Haldemann A. F. C., Klingelhoefer G., Ming D. W., Morris R. V., de Souza P. A., Squyres S. W., Weitz C., Yen A. S., Zipfel J., and Economou T. 2008. Meteorites on Mars observed with the Mars Exploration Rovers. *Journal of Geophysical Research-Planets* 113: E06S22. doi:10.1029/2007JE002990.

Sierks H., Lamy P., Barbieri C., Koschny D., Rickman H., Rodrigo R., A'Hearn M. F., Angrilli F., Barucci M. A., Bertaux J. L., Bertini I., Besse S., Carry B., Cremonese G., Da Deppo V., Davidsson B., Debei S., De Cecco M., De Leon J., Ferri F., Fornasier S., Fulle M., Hviid S. F., Gaskell R. W., Groussin O., Gutierrez P., Ip W., Jorda L., Kaasalainen M., Keller H. U., Knollenberg J., Kramm R., Kuhrt E., Kuppers M., Lara L., Lazzarin M., Leyrat C., Moreno J. J. L., Magrin S., Marchi S., Marzari F., Massironi M., Michalik H., Moissl R., Naletto G., Preusker F., Sabau L., Sabolo W., Scholten F., Snodgrass C., Thomas N., Tubiana C., Vernazza P., Vincent J. B., Wenzel K. P., Andert T., Patzold M., and Weiss B. P. 2011. Images of Asteroid 21 Lutetia: A remnant planetesimal from the early solar System. *Science* 334:487–490.

Takeda H., Mori H., Hiroi T., and Saito J. 1994. Mineralogy of new Antarctic achondrites with affinity to Lodran and a model of their evolution in an asteroid. *Meteoritics* 29:830–842.

Trombka J. I., Squyres S. W., Bruckner J., Boynton W. V., Reedy R. C., McCoy T. J., Gorenstein P., Evans L. G., Arnold J. R., Starr R. D., Nittler L. R., Murphy M. E., Mikheeva I., McNutt R. L., McClanahan T. P., McCartney E., Goldsten J. O., Gold R. E., Floyd S. R., Clark P. E., Burbine T. H., Bhangoo J. S., Bailey S. H., and Petaev M. 2000. The elemental composition of asteroid 433 Eros: Results of the NEAR-Shoemaker X-Ray Spectrometer. *Science* 289:2101–2105.

Tsuda Y., Yoshikawa M., Abe M., Minamino H., and Nakazawa S. 2013. System design of the Hayabusa 2-Asteroid sample return mission to 1999 JU3. *Acta Astronautica* 91:356–362.

Urey H. C. and Craig H. 1953. The composition of the stone meteorites and the origin of the meteorites. *Geochimica et Cosmochimica Acta* 4:36–82.

Veverka J., Belton M., Klaasen K., and Chapman C. 1994. Galileo encounter with 951-Gaspra—Overview. *Icarus* 107:2–17.

Veverka J., Thomas P. C., Robinson M., Murchie S., Chapman C., Bell M., Harch A., Merline W. J., Bell J. F., Bussey B., Carcich B., Cheng A., Clark B., Domingue D., Dunham D., Farquhar R., Gaffey M. J., Hawkins E., Izenberg N., Joseph J., Kirk R., Li H., Lucey P., Malin M., McFadden L., Miller J. K., Owen W. M., Peterson C., Prockter L., Warren J., Wellnitz D., Williams B. G., and Yeomans D. K. 2001. Imaging of small-scale features on 433 Eros from NEAR: Evidence for a complex regolith. *Science* 292:484–488.

Ward J. H Jr. 1963. Hierarchical grouping to optimize an objective function. *Journal of the American Statistical Association* 58: 236–244.

Weisberg M. K., McCoy T. J., and Krot A. N. 2006. Systematics and evaluation of meteorite classification. In *Meteorites and the early solar system II*, edited by Lauretta D. S. and McSween H. Y. Tucson, Arizona: University of Arizona Press. pp. 19–53.

Yanai K. and Kojima H. 1995. *Catalog of Antarctic meteorites*. Tokyo: National Institute of Polar Research.

Yano H., Kubota T., Miyamoto H., Okada T., Scheeres D., Takagi Y., Yoshida K., Abe M., Abe S., Barnouin-Jha O., Fujiwara A., Hasegawa S., Hashimoto T., Ishiguro M., Kato M., Kawaguchi J., Mukai T., Saito J., Sasaki S., and Yoshikawa M. 2006. Touchdown of the Hayabusa spacecraft at the Muses Sea on Itokawa. *Science* 312:1350–1353.

Zolensky M. and Ivanov A. 2003. The Kaidun microbreccia meteorite: A harvest from the inner and outer asteroid belt. *Chemie Der Erde-Geochemistry* 63:185–246.

Zolensky M. E., Zega T. J., Yano H., Wirick S., Westphal A. J., Weisberg M. K., Weber I., Warren J. L., Velbel M. A., Tsuchiyama A., Tsou P., Toppani A., Tomioka N., Tomeoka K., Teslich N., Taheri M., Susini J., Stroud R., Stephan T., Stadermann F. J., Snead C. J., Simon S. B., Simionovici A., See T. H., Robert F., Rietmeijer F. J. M., Rao W., Perronnet M. C., Papanastassiou D. A., Okudaira K., Ohsumi K., Ohnishi I., Nakamura-Messenger K., Nakamura T., Mostefaoui S., Mikouchi T., Meibom A., Matrajt G., Marcus M. A., Leroux H., Lemelle L., Le L., Lanzirotti A., Langenhorst F., Krot A. N., Keller L. P., Kearsley A. T., Joswiak D., Jacob D., Ishii H., Harvey R., Hagiya K., Grossman L., Grossman J. N., Graham G. A., Gounelle M., Gillet P., Genge M. J., Flynn G., Ferroir T., Fallon S., Ebel D. S., Dai Z. R., Cordier P., Clark B., Chi M. F., Butterworth A. L., Brownlee D. E., Bridges J. C., Brennan S., Brearley A., Bradley J. P., Bleuet P., Bland P. A., and Bastien R. 2006. Report—Mineralogy and petrology of comet 81P/Wild 2 nucleus samples. *Science* 314:1735–1739.

Zolensky M., Mikouchi T., Fries M., Bodnar R., Jenniskens P., Yin Q. Z., Hagiya K., Ohsumi K., Komatsu M., Colbert M., Hanna R., Maisano J., Ketcham R., Kebukawa Y., Nakamura T., Matsuoka M., Sasaki S., Tsuchiyama A., Gounelle M., Le L., Martinez J., Ross K., and Rahman Z. 2014. Mineralogy and petrography of C asteroid regolith: The Sutter's Mill CM meteorite. *Meteoritics & Planetary Science* 49:1997–2016.

SUPPORTING INFORMATION

Additional supporting information may be found in the online version of this article:

Fig S1. Full-scale version of Figure 1. Dendrogram resulted from the hierarchical clustering analysis of elementary composition database of NIPR meteorites by Ward method based on 12 elements.